BIOCHEMISTRY
including biophysical chemistry & molecular biology
Article

Biochemistry **2010,** *49,* 4833–4840 4833
DOI: 10.1021/bi100200c

Incorporation of Gemcitabine and Cytarabine into DNA by DNA Polymerase β and Ligase III/XRCC1[†]

A. S. Prakasha Gowda,[‡] Joanna M. Polizzi,[‡] Kristin A. Eckert,[§] and Thomas E. Spratt*,[‡]

[‡]*Department of Biochemistry and Molecular Biology and* [§]*Department of Pathology, The Pennsylvania State University, Hershey, Pennsylvania 17033*

Received February 9, 2010; Revised Manuscript Received May 7, 2010

ABSTRACT: 1-β-D-Arabinofuranosylcytosine (cytarabine, araC) and 2′,2′-difluoro-2′-deoxycytidine (gemcitabine, dFdC), are effective cancer chemotherapeutic agents due to their ability to become incorporated into DNA and then subsequently inhibit DNA synthesis by replicative DNA polymerases. However, the impact of these 3′-modified nucleotides on the activity of specialized DNA polymerases has not been investigated. The role of polymerase β and base excision repair may be of particular importance due to the increased oxidative stress in tumors, increased oxidative stress caused by chemotherapy treatment, and the variable amounts of polymerase β in tumors. Here we directly investigate the incorporation of the 5′-triphosphorylated form of araC, dFdC, 2′-fluoro-2′-deoxycytidine (FdC), and cytidine into two nicked DNA substrates and the subsequent ligation. Opposite template dG, the relative k_{pol}/K_d for incorporation was dCTP > araCTP, dFdCTP ≫ rCTP. The relative k_{pol}/K_d for FdCTP depended on sequence. The effect on k_{pol}/K_d was due largely to changes in k_{pol} with no differences in the affinity of the nucleoside triphosphates to the polymerase. Ligation efficiency by T4 ligase and ligase III/XRCC1 was largely unaffected by the nucleotide analogues. Our results show that BER is capable of incorporating araC and dFdC into the genome.

Nucleoside analogues are an important class of cancer chemotherapeutics that are used for the treatment of various malignancies. Two drugs of this class, 1-β-D-arabinofuranosylcytosine (cytarabine, araC)[1] and 2′,2′-difluoro-2′-deoxycytidine (gemcitabine, dFdC), are analogues of 2′-deoxycytidine (dC) (Chart 1). AraC is successful in the treatment of acute myeloid leukemia and hematological malignances (*1*). Gemcitabine is successfully used as a single agent or in combination chemotherapy in the treatment of non-small cell lung (*2*), pancreatic (*3*, *4*), ovarian (*5*), and breast cancer (*6*, *7*), as well as in the treatment of hematological malignancies (*8*). Gemcitabine has also shown promising efficacy for the treatment of other malignancies (*9*), suggesting more widespread use in the future. In addition to its use as a monotherapy, gemcitabine is often most effective when used as part of a combination therapy, frequently with platinum-based and topoisomerase-targeted chemotherapeutic agents.

The mechanism of action of each drug is multifaceted but primarily involves inhibiting DNA synthesis (*10*−*12*). Both araC and dFdC are transported into the cell where they are activated by phosphorylation (*10*, *13*). 2′,2′-Difluoro-2′-deoxycytidine 5′-diphosphate (dFdCDP) is a potent inhibitor of ribonucleotide reductase (*14*−*16*), which will lower dNTP pools and lead to inhibition of DNA synthesis. The triphosphates of dFdC and araC are incorporated into DNA opposite dG but then inhibit DNA synthesis. When araC and dFdC are incorporated into DNA, they are also potent inhibitors of topoisomerase I (*17*, *18*).

In vitro primer extension reactions with DNA polymerases α (pol α) and ε (pol ε) have shown that araCTP and dFdCTP inhibit DNA synthesis by becoming incorporated into the DNA and then inhibiting DNA synthesis (*10*, *11*, *19*) as illustrated in Scheme 1A. Steady-state studies found that pol ε and pol α incorporate dFdCTP 20−80-fold less efficiently than dCTP (*11*, *19*). Inhibition by araC occurs immediately after araC incorporation, while dFdC inhibits via a masked termination mechanism in which, after dFdC incorporation, an additional nucleotide is incorporated after which DNA synthesis is inhibited. It is thought that the addition of a correct base pair prevents the proofreading exonuclease activity of DNA pol ε to remove dFdCMP once incorporated into DNA (*11*). The effect of the inhibition varies with polymerase. AraC and dFdC inhibit pol α and pol ε more than DNA polymerase δ (*20*). Inhibition of DNA synthesis by dFdC by the masked termination mechanism is not a universal mechanism. While the mammalian B-family polymerases are inhibited by dFdC via the masked termination mechanisms, pol γ is not (*21*).

While the replicative polymerases synthesize the vast majority of DNA in a cell, there is evidence that specialized polymerases play a role in the incorporation of these nucleotide analogues into the DNA. Gemcitabine induces S-phase arrest (*22*) and stalls replication forks and induces H2AX phosphorylation (*23*), events that signal the action of translesion DNA polymerases to rescue stalled replication forks. In addition, the cytotoxic effects of araC and dFdC are dependent on the activity of the translesion DNA polymerase η (*24*, *25*). These results suggest that translesion bypass polymerases play a role in the incorporation of these nucleoside analogues into the DNA. In addition, DNA repair polymerases also appear to be important in the cytotoxicity of araC and dFdC. For example, the a major route of incorporation of araC into the genome is through DNA replication accompanying DNA repair (*12*). Furthermore, gemcitabine is slightly less

[†]This project is funded, in part, under a grant with the Pennsylvania Department of Health using Tobacco Settlement Funds.

*To whom correspondence should be addressed: telephone, 717-531-4623; fax, 717-531-7072; e-mail, tes13@psu.edu.

[1]Abbreviations: araC, 1-β-D-arabinofuranosylcytosine; BER, base excision repair; dFdC, 2′,2′-difluoro-2′-deoxycytidine; DTT, dithiothreitol; dNTP, 2′-deoxynucleoside 5′-triphosphate; FdC, 2′-fluoro-2′-deoxycytidine; PAGE, polyacrylamide gel electrophoresis; pol, polymerase; SDS, sodium dodecyl sulfate.

Published on Web 05/12/2010

Chart 1: Structures of 2′-Deoxycytidine (dC), 1-β-D-Arabino-furanosylcytosine (araC), Cytidine (rC), 2′-Fluoro-2′-deoxycytidine (FdC), and 2′,2′-Difluoro-2′-deoxycytidine (dFdC)

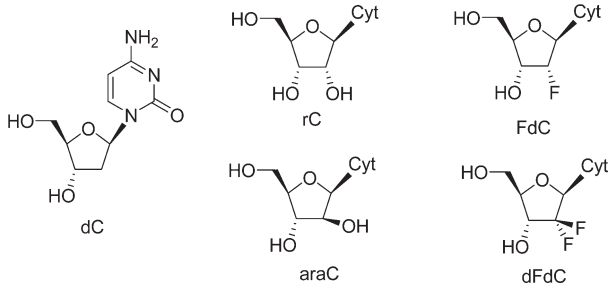

Scheme 1

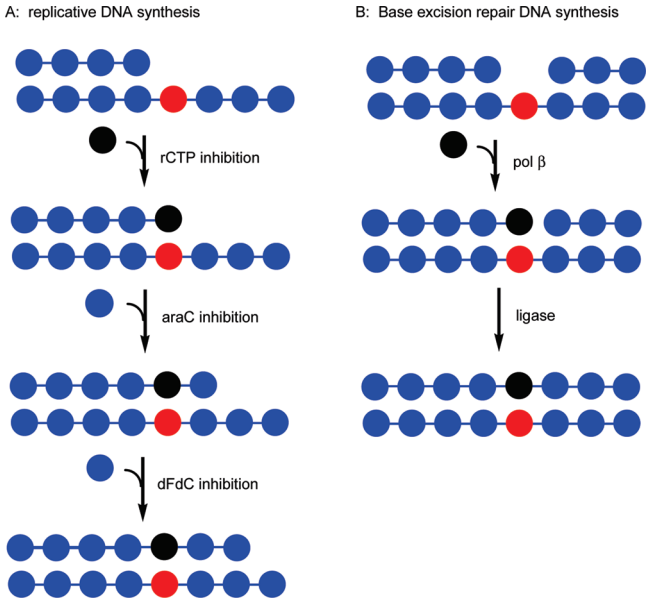

toxic to BER-deficient cells, suggesting that DNA polymerase β (pol β) may be responsible for some of gemcitabine's toxicity (*26*). The increased oxidative stress of the tumor (*27*−*29*) and the induction of oxidative stress by the chemotherapeutic regimen (*2*, *5*, *30*, *31*) may also lead to the incorporation of araC and dFdC via BER (*33*). In addition, several tumor types, including kidney, breast, prostate, uterus, ovary, colon, lung, stomach, and rectum, have even been shown to have increased expression of pol β (*32*).

In this report, we have evaluated the potential of incorporation of araC and dFdC via the base excision repair (BER) pathway. During BER, DNA damage is recognized and excised by DNA glycosylases and/or endonucleases leaving behind a gap in the DNA that is filled by DNA pol β and then sealed by DNA ligase III/XRCC1, as illustrated in Scheme 1B. This pathway bypasses the traditional and masked chain termination mechanisms of these drugs and may provide an efficient pathway or the incorporation of the drugs into the genome.

MATERIALS AND METHODS

Reagents. T4 polynucleotide kinase was purchased from Epicenter (Lexington, KY) and [γ-^{32}P]ATP (6000 Ci/mmol) from Perkin-Elmer (Waltham, MA). T4 ligase was purchased from New England Biolabs. The concentration was determined kinetically as described (*33*, *34*). Human ligase III and XRCC1 were purchased from Enzymax (Lexington, KY). DNA oligomers were purchased from IDT (San Jose, CA). The nucleoside

Chart 2: DNA Substrates

DNA-1
5′-CTACTGCGGGTTTAGAT GTCGGTCCGCACGGC-3′
3′-GATGACGCCCAAATCTAGCAGCCAGGCGTGCCG-5′

DNA-2
5′-CTACTGCGGGTTTAGATX GTCGGTCCGCACGGC-3′
3′-GATGACGCCCAAATCTAG−CAGCCAGGCGTGCCG-5′

DNA-3
5′- GAAGACTGGTGAAGACTTGAG TACAGGTCGATTCATGG-3′
3′-ACTTCTGACCACTTCTGAACTCGATGTCCAGCTAAGTACC-5′

DNA-4
5′- GAAGACTGGTGAAGACTTGAGX TACAGGTCGATTCATGG-3′
3′-ACTTCTGACCACTTCTGAACTCG−ATGTCCAGCTAAGTACC-5′

triphosphates, dCTP and rCTP, were purchased from Promega (Madison, WI). Modified nucleoside triphosphates, araCTP and FdCTP, were purchased from Trilink Biotechnologies (San Diego, CA). Gemzar (Eli Lilly and Co., Indianapolis, IN) was purchased from the Outpatient Pharmacy at the Penn State Hershey Medical Center. Gemcitabine was converted to the triphosphate by the procedure described by Ludwig (*35*) as described in the Supporting Information. The concentrations of the dNTPs were each determined by UV absorbance (*41*).

Generation and Purification of Histidine-Tagged Polymerase β. Protein expression and purification were performed as previously described (*36*). Dr. Joann Sweasy (Yale University, New Haven, CT) supplied the cDNA of WT polymerase β which was subcloned behind an N-terminal hexahistidine tag in the pET28a vector and transformed into BL21-λDE3 *Escherichia coli* cells. Purity was confirmed by SDS−PAGE as shown in the Supporting Information.

DNA Substrates. The DNA substrates contain a template, a primer, and a downstream blocking oligodeoxynucleotide as illustrated in Chart 2. The primer strands were 5′-end-labeled with ^{32}P using T4 polynucleotide kinase and [γ-^{32}P]ATP (6000 Ci/mmol) as previously described (*37*). The blocking strands were phosphorylated on the 5′-end with nonradioactive ATP. The unreacted [γ-^{32}P]ATP and ATP were removed using a G-25 spin column and annealed at a primer:blocker:template ratio of 1:3:1.

Steady-State Kinetic Experiments. Reactions were performed in pol β reaction buffer (50 mM Tris-HCl (pH 7.5), 100 mM NaCl, 100 μg/mL BSA, 1 mM DTT, 5 mM $MgCl_2$) and various concentrations of dNTPs at 37 °C. The reactions were initiated by the addition of dNTP and $MgCl_2$ to DNA polymerase β and a radiolabeled gapped DNA substrate. The DNA concentration was 10 nM, the dNTP concentrations ranged from 0.01 to 1000 μM, and DNA polymerase β concentrations ranged from 0.1 to 1 nM. Reactions were quenched at various times with STOP solution consisting of 10% 300 mM EDTA (pH 8.0) and 90% formamide containing 0.025% (w/v) bromophenol blue and 0.025% (w/v) xylene cyanol.

Pre-Steady-State Kinetic Experiments. A KinTek-3 rapid quench apparatus was used to perform experiments ranging in time from 2 ms to 60 s at 37 °C in pol β reaction buffer and various concentrations of dNTP. The reactions were initiated by the addition of dNTP and $MgCl_2$ to DNA polymerase β and a radiolabeled single nucleotide gapped DNA substrate. During the burst reactions, the final concentrations of DNA and polymerase were 40 and 10 nM, respectively. During the single-turnover experiments, the final concentrations of DNA and

Table 1: Kinetic Parameters for DNA Polymerase β Catalyzed Incorporation of dCTP and Analogues into DNA

	steady-state parameters			single-turnover parameters		
dNTP	k_{cat} (s^{-1})	K_m (μM)	k_{cat}/K_m (M^{-1} s^{-1})	k_{pol} (s^{-1})	K_d (μM)	k_{pol}/K_d (M^{-1} s^{-1})
			DNA Substrate: DNA-1			
dCTP	0.12 ± 0.01	0.50 ± 0.14	240000	4.6 ± 1.9	18 ± 6	256000
dFdCTP	0.12 ± 0.01	24 ± 07	5100	1.4 ± 0.2	36 ± 21	38900
araCTP	0.103 ± 0.005	6 ± 4	27000	1.0 ± 0.1	26 ± 6	38500
FdCTP	0.015 ± 0.0009	12 ± 2	1400	1.4 ± 0.07	27 ± 2	52000
rCTP	0.015 ± 0.001	175 ± 29	84	0.0020 ± 0.0001	30 ± 6	67
			DNA Substrate: DNA-3			
dCTP	0.12 ± 0.03	0.52 ± 0.02	230000	3.5 ± 0.2	7.8 ± 0.2	450000
dFdCTP	0.0018 ± 0.001	24 ± 4	75	0.66 ± 0.5	14.4 ± 6.6	46000
araCTP	0.0025 ± 0.001	12 ± 2	210	0.95 ± 0.03	9.7 ± 1.7	98000
FdCTP	0.0051 ± 0.0003	51 ± 3	100	0.0029 ± 0.0001	16 ± 3	180
rCTP	0.0031 ± 0.0003	31 ± 12	100	0.0017 ± 0.0001	10 ± 4	170

polymerase were 10 and 40 nM, respectively. Reactions were quenched with 300 mM EDTA (pH 8.0).

Ligation Assay. The nicked DNA substrates (DNA-2 and DNA-4) were created by incubating a 5′-^{32}P-labeled single nucleotide gapped DNA substrate with DNA polymerase β and 200 μM dNTP at 37 °C in pol β reaction buffer for at least 15 min. The T4 ligase or ligase III/XRCC1 was preincubated with ATP for 15 min in T4 reaction buffer (33 mM Tris−acetate (pH 7.8), 66 mM potassium acetate, 10 mM magnesium acetate, and 0.5 mM DTT) or ligase III/XRCC1 reaction buffer (50 mM Tris-HCl (pH 7.4), 20 mM NaCl, 1 mM DTT, and 10 mM $MgCl_2$). The newly formed nicked DNA substrate was subsequently reacted with ligase in the appropriate reaction buffer. The reactions were quenched with STOP solution.

Product Analysis by Polyacrylamide Gel Electrophoresis (*PAGE*). The reaction products were separated on a denaturing PAGE in 15% acrylamide (19:1 acrylamide:*N*,*N*′-methylenebisacrylamide) and 7 M urea in 89 mM Tris, 89 mM boric acid, and 2 mM Na_2EDTA. The size of the gel was 40 cm × 33 cm × 0.4 cm and was run at 2000 V for 2−2.5 h. The gel was visualized and quantified using a Typhoon 9200 phosphoimager with ImageQuant software. The progress of the reaction was quantitated by dividing the total radioactivity of the product band by the radioactivity of the product and reactant bands.

Data Analysis. Data were fitted by nonlinear regression using Prism version 4 for Windows (GraphPad Software, San Diego, CA; www.graphpad.com). Steady-state parameters were determined by fitting the data to eq 1, where v_0 is the initial rate, E is the polymerase, and K_m is the Michaelis constant for the dNTP.

Data from the burst reactions were fitted to eq 2 in which P is the total product formed, k the burst rate constant, k_{ss} the steady-state rate constant, A the burst amplitude, and t time. The dissociation constant of the DNA, K_d^{DNA} was determined by fitting the burst amplitude A versus the polymerase concentration [E] to eq 3 in which [D] is the concentration of the DNA. The single-turnover experiments were fitted to eq 4 in which P is the amount of product formed, A the amplitude of the reaction, and k the first-order rate constant for the incorporation of dNTP. The k determined for each concentration was then fit to a hyperbolic equation (eq 5), where k_{pol} is the maximum k of dNTP incorporation and K_d^{dNTP} is the dissociation constant for the dNTP with the polymerase−DNA complex.

The observed rates (k) for the ligase III/XRCC1 and the T4 ligase reactions were calculated using the first-order equation (eq 4).

$$\frac{v_0}{[E]_0} = \frac{k_{cat}[dNTP]_0}{K_m + [dNTP]_0} \quad (1)$$

$$P = A(1 - e^{-kt}) + k_{ss}t \quad (2)$$

$$A = \frac{([D] + [E] + K_d^{DNA}) - \sqrt{([D]+[E]+K_d^{DNA})^2 - 4[E][D]}}{2} \quad (3)$$

$$P = A(1 - e^{-kt}) \quad (4)$$

$$k = \frac{k_{pol}[dNTP]_0}{K_d^{dNTP} + [dNTP]_0} \quad (5)$$

RESULTS

Steady-State DNA Polymerase Kinetics. The incorporation of dCTP, rCTP, araCTP, FdCTP, and dFdCTP into the two single nucleotide gapped substrates DNA-1 and DNA-3 pol β was examined under steady-state conditions. The results are summarized in Table 1. In both sequences, the k_{cat}/K_m for rCTP was 3 orders of magnitude less than that of dCTP, similar to previous results (*38*, *39*). We found that the reduced k_{cat}/K_m was due to a decrease in k_{cat} as well as an increase in K_m as was found previously (*38*). The k_{cat}/K_m for araCTP and dFdCTP was 5−40-fold less than dCTP in DNA-1 but 1200−2400-fold less with DNA-3. In both sequence contexts, the K_m for dCTP was much lower than that for the analogues, but in DNA-1 the k_{cat} values for the analogues were equivalent to that of dCTP, while in DNA-3, the k_{cat} for dFdCTP and araCTP were decreased ~50-fold versus dCTP. The kinetics of incorporation of FdCTP also depended on sequence. In the DNA-1 context, FdCTP was incorporated as rapidly as araCTP and dFdCTP while with DNA-3, the rate was as slow as rCTP. To gain a greater understanding of the mechanism, we evaluated the reaction under single-turnover conditions.

Pre-Steady-State DNA Polymerase Kinetics. The polymerase kinetic scheme is quite complex, and the steady-state kinetic parameters cannot be assigned to individual steps. The K_m

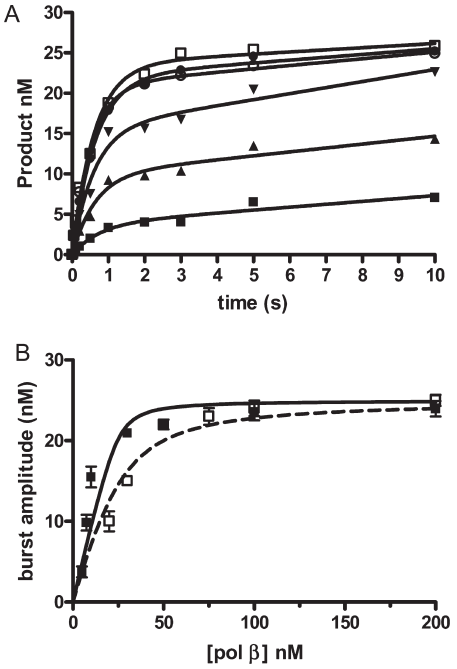

FIGURE 1: Determination of the K_d^{DNA}. (A) Reaction of 100 μM dCTP and 25 nM DNA-3 with 5 (■), 7.5 (▲), 10 (▼), 30 (○), 50 (●), and 100 (□) nM pol β. The lines are the best fit to eq 2. (B) Determination of K_d^{DNA}. The burst amplitudes for DNA-1 (□) and DNA-3 (■) are plotted against concentration of pol β. The points are the mean ± standard deviation of three determinations. The lines are the best fit to eq 3 for DNA-1 (- - -) and DNA-3 (—).

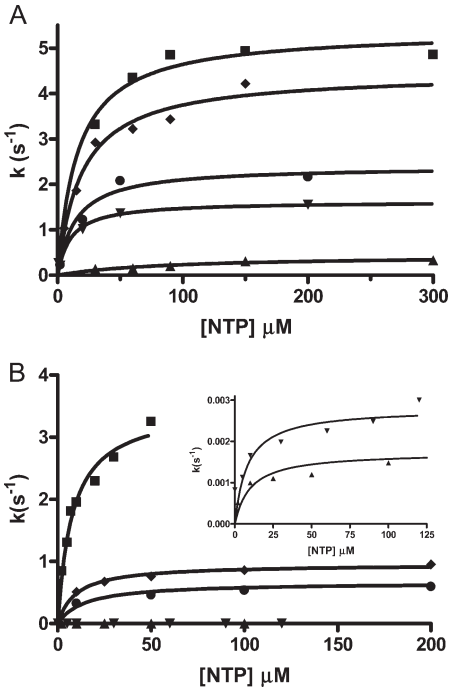

FIGURE 2: Determination of k_{pol} and K_d^{dNTP}. Plot of first-order rate constant (k) versus concentration of NTP for reaction between 40 nM pol β and 10 nM (A) DNA-1 and (B) DNA-3. The triphosphates are represented by the symbols dCTP (■), araCTP (◆), FdCTP (▼), dFdCTP (●), and rCTP (▲). The solid lines are the best fit to eq 5. The insert in panel B shows the data for dFdCTP and rCTP with an expanded Y-axis.

parameter is especially difficult to interpret. To gain a better understanding of the mechanism underlying the selectivity at the 2′-position, we analyzed the incorporation with single-turnover kinetics. Under these conditions, the rate-limiting step is phosphodiester bond formation (*40*−*42*).

The K_d^{DNA} was determined as illustrated in Figure 1. The burst amplitudes were determined at various concentrations of pol β at constant DNA concentrations. The time course data were fitted to eq 2. The burst amplitude was then plotted against the concentration of pol β and fitted to eq 3. The K_d^{DNA} was determined to be 7.5 ± 1.8 nM for DNA-1 and 1.4 ± 0.7 for DNA-3. While the percent error in the error in the K_d^{DNA} for DNA-3 is large, the overall conclusion is that the DNA is tightly bound to the polymerase with both sequences.

The ability of DNA polymerase β to incorporate dCTP and its analogues into a gapped DNA substrate was further characterized using single-turnover kinetic studies in which enzyme was used in a 4-fold excess over DNA. These concentrations were employed to ensure that the reactions went to > 80% completion with dCTP. The time courses were fitted to eq 4 and first-order rate constants determined. The first-order rate constants were plotted against triphosphate concentration and fitted to eq 5 as illustrated in Figure 2. The k_{pol} and K_d^{NTP} values are listed in Table 1. The k_{pol} and K_d^{NTP} values for dCTP are similar to those determined previously (*43*, *44*).

For both sequences, the selectivity against rCTP incorporation was 3 orders of magnitude. The differences in rate between dCTP and rCTP are due to decreased rate of phosphodiester bond formation (k_{pol}), not binding affinity of the nucleoside triphosphate (K_d^{NTP}). This observation differs slightly from *E. coli* DNA polymerase I (exo$^-$) in which while ribose discrimination is primarily due to a decrease in k_{pol}, the ribose triphosphate binds 10-fold less effectively than the dNTP (*45*).

In DNA-1, the decreased k_{cat}/K_m for araC and dFdC are due to increased K_m values. The single-turnover experiments demonstrated that the increased K_m values were due to up to 2-fold increases in K_d^{dNTP} and ~4-fold decreases in rates of phosphodiester bond formation (k_{pol}). The decreased rate of phosphodiester bond formation is not reflected in the k_{cat} parameter because the dissociation of the DNA from the polymerase is rate limiting, which is typical of DNA polymerases. In contrast, with DNA-3, the larger decreases in k_{cat}/K_m are due to increased K_m values as with DNA-1 as well as decreased k_{cat} values. The single-turnover experiments indicate that the rates of phosphodiester bond formation are rapid, similar to those with DNA-1. The small increases in K_d^{NTP} and decreases in k_{pol} can account for the increase in K_m for dFdCTP and araCTP with DNA-3. The reduction in k_{cat} is independent from the binding and catalytic steps and may be due to a decrease in the rate of dissociation of the DNA from the polymerase.

A reduced rate of the dissociation of the DNA from the polymerase was investigated further by the experiments in Figure 3 in which the incorporation of dCTP, araCTP, and dFdCTP into DNA-3 was performed with 50 nM DNA and 10 nM pol β. The time course data show the formation of product is two phase in which the initial first-order burst is followed by a linear steady-state formation of product that can be fitted to eq 2. The burst rates for dCTP (2.6 s^{-1}), araCTP (0.47 s^{-1}), and dFdCTP (0.23 s^{-1}) are similar to those found for the k_{pol} values shown in Table 1. The burst amplitudes are all approximately 10 nM and equal to the polymerase concentration. The steady-state rates differ, with the k_{ss} for dCTP (1.0 nM s^{-1}) much greater than those for araCTP (0.026 nM s^{-1}) and dFdCTP (0.026 nM s^{-1}). As the $k_{ss} = k_{cat}$[pol β], these k_{ss} values are consistent with the k_{cat} values shown in Table 1. The results indicate that the difference in

sequence causes differences in the rate of dissociation of the DNA from the polymerase.

Ligation. During BER, after pol β incorporates dFdC and araC into the DNA, the product must be ligated. We examined the ability of araC and dFdC to be ligated using T4 ligase I and human ligase III/XRCC1. The nicked substrates for the ligation experiments were synthesized *in situ* by incubating pol β and NTP with the single nucleotide gapped substrates DNA-1 and DNA-3 to produce DNA-2 and DNA-4. The ability of the products of the pol β reactions to be ligated was initially evaluated with T4 ligase. The ligation was monitored by PAGE as illustrated in Figure 4. The ligation was performed using enzyme in excess over DNA (40 nM T4 ligase and 10 nM DNA) and was analyzed by first-order kinetics (eq 4). The first-order rate constants are listed in Table 2. Ligation was rapid for DNA-2 but was 50-fold slower for DNA-4. The identity of the nucleotide does not significantly influence the reaction rate. The maximum rate reduction was 5-fold with dFdC in DNA-2. Previously, it was found that araC was ligated approximately 3-fold more slowly than dC when placed at the 3′-terminus (*46*). We found that araC affected the rate of incorporation minimally.

To gain a better understanding of what may be occurring in humans, we examined the ability of the ligase III/XRCC1 complex to seal the nicked DNA substrates. Ligation was performed as described above with a 4-fold excess of ligase III/XRCC1 over DNA. The results show that the rate of ligation with dC by ligase III/XRCC1 was less affected by DNA sequence than T4 ligase; DNA-2 was ligated 4-fold faster than DNA-4. As with T4 ligase, the identity of the nucleotide at the 3′-terminus did not significantly affect the rate of ligation. In DNA-2, the rate of ligation with dFdC was reduced 10-fold, and the rate of ligation with araC was reduced 60-fold. However in DNA-4, dFdC did not affect the rate of ligation while araC slowed down ligation only 3-fold (Figure 5).

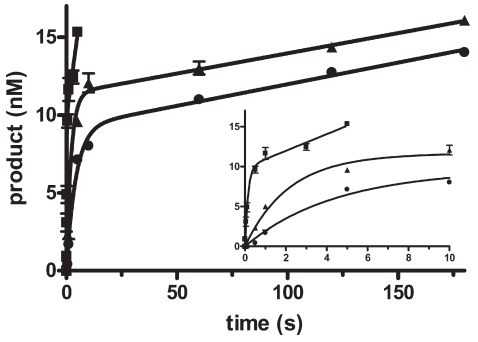

FIGURE 3: Burst kinetics for the incorporation of dCTP (■), araCTP (▲), and dFdCTP (●) into DNA-3 with 10 nM pol β, 50 nM DNA-3, and 100 μM NTP. The insert shows the time course up to 10 s. Each data point is the mean of three determinations, and the error bars represent the standard deviations. The line is the best fit curve to eq 2 with the following parameters: dCTP, $A = 9.8$ nM, $k = 6.8\ s^{-1}$, $k_{ss} = 1.0$ nM s^{-1}; araCTP, $A = 11$ nM, $k = 0.47\ s^{-1}$, $k_{ss} = 0.026$ nM s^{-1}; dFdCTP, $A = 9.2$ nM, $k = 0.23\ s^{-1}$, $k_{ss} = 0.026$ nM s^{-1}.

DISCUSSION

DNA Polymerase β. The DNA polymerase kinetic mechanism consists of multiple steps that can be visualized by a variety of techniques and experimental protocols (*41*, *42*, *47*, *48*). Under single-turnover conditions, phosphodiester bond formation is rate limiting for both correct and mispair formation (*41*, *42*, *47*). Under multiple-turnover conditions, however, dissociation of the DNA from the polymerase is rate limiting. We found that the 2′-ribose substitutions have a variable effect on pol β catalyzed incorporation. As previously documented (*38*, *39*), we also found rCTP to be a poor substrate, with k_{cat}/K_m and k_{pol}/K_d^{dNTP} values 3 orders of magnitude less than that of dCTP. We found that the hydroxyl substitution causes the large decrease in the rate of phosphodiester bond formation but does not significantly affect the binding of the triphosphate to the polymerase. The rate of phosphodiester bond formation is rate limiting in both single- and multiple-turnover reactions for rCTP. araCTP and dFdCTP are relatively good substrates in spite of the substitutions at the 2′-positions. The rate of phosphodiester bond formation is decreased approximately 5-fold in both DNA-1 and DNA-3. However, with DNA-3, the rate of product dissociation is much slower with araC and dFdC incorporated in the DNA. The rate of phosphodiester bond formation with FdCTP varied with sequence. In DNA-1, it was only 4-fold less than that of dCTP while in DNA-3, it was as poor a substrate as rCTP.

High-fidelity DNA polymerases use steric interactions on the minor groove side of the ribose to select against ribonucleoside triphosphate incorporation. These interactions are via side chains in the A-, B-, and Y-families as well as with HIV-RT (*45*, *49*−*54*). Crystallography experiments have suggested that pol β selects against ribose incorporation through steric exclusion by the protein backbone segment spanning Tyr271 to Gly274 (*55*, *56*). The mechanisms of ribose exclusion of two X-family polymerases have been examined. Pol μ, an X-family polymerase that readily incorporates rNTPs, has a Gly at the position that corresponds to Tyr271 in pol β. Changing the Gly to Tyr created a polymerase (G433Y) that effectively discriminates against rNTPs (*39*). The mechanism by which pol λ discriminates against rNTP incorporation is more

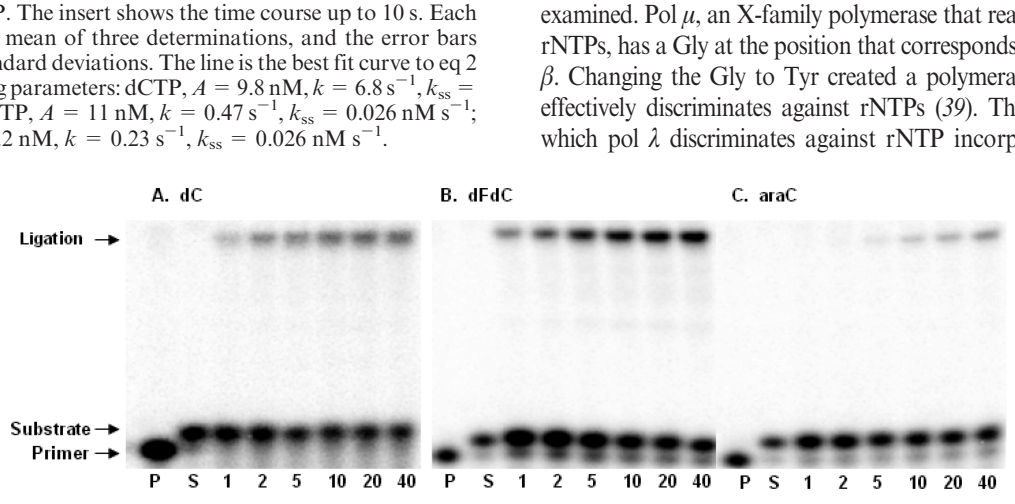

FIGURE 4: Ligation by the ligase III/XRCC1 complex. Single gapped DNA (5 nM) and polymerase β (1 nM) were reacted with 200 μM (A) dCTP, (B) dFdCTP, and (C) araCTP to form a nicked DNA substrate in 50 mM Tris-HCl (pH 7.5), 100 mM NaCl, 0.1 mM EDTA, 1 mM DTT, 5 mM $MgCl_2$, and 100 μg/mL BSA. P is 17-mer primer and S is nicked DNA substrate. The nicked DNA (2.5 nM) substrate was then incubated with 10 nM ligase III/XRCC1 complex at 37 °C. The reactions were quenched with EDTA at 1, 2, 5, 10, 20, and 40 min, and the reactants and products were resolved by PAGE and analyzed by phosphorimaging.

Table 2: Rates for T4 Ligase and Ligase III/XRCC1 Catalyzed Nick Sealing of dCMP and Analogues

	DNA-2		DNA-4	
X	T4 ligase[a] k_{obs} (min^{-1})	ligase III/XRCC1[b] k_{obs} (min^{-1})	T4 ligase[a] k_{obs} (min^{-1})	ligase III/XRCC1[b] k_{obs} (min^{-1})
dC	16 ± 4	0.8 ± 0.1	0.20 ± 0.02	0.21 ± 0.01
dFdC	3.1 ± 0.7	0.08 ± 0.01	0.15 ± 0.02	0.27 ± 0.03
araC	12 ± 3	0.014 ± 0.002	0.15 ± 0.02	0.077 ± 0.008
FdC	10 ± 3	0.34 ± 0.04	0.24 ± 0.03	0.27 ± 0.03
rC	9 ± 2	0.38 ± 0.04	0.26 ± 0.03	0.46 ± 0.03

[a]10 nM DNA, 40 nM T4 ligase, and 2 mM ATP. [b]10 nM DNA, 10 nM ligase III, 10 nM XRCC1, and 2 mM ATP.

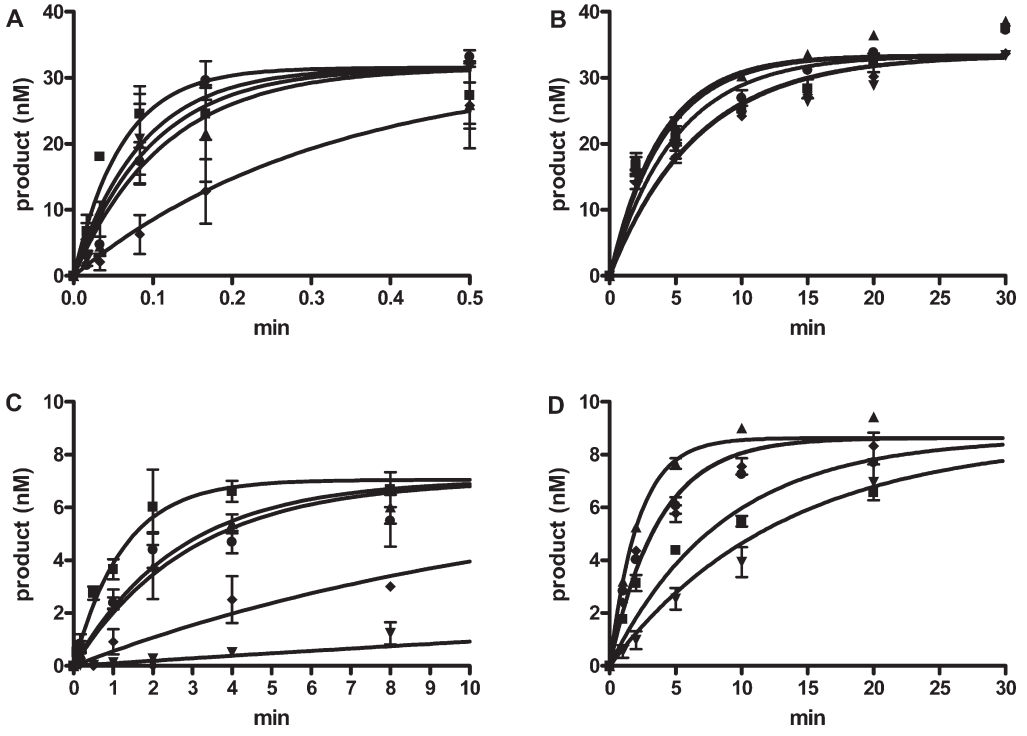

FIGURE 5: Time course for ligation of DNA-2 and DNA-4 containing dC (■), araC (▼), FdC (●), dFdC (◆), or rC (▲). Reaction between (A) 200 nM T4 ligase and 40 nM DNA-2, (B) 200 nM T4 ligase and 40 nM DNA-4, (C) 40 nM ligase III/XRCC1 and 10 nM DNA-2, and (D) 40 nM ligase III/XRCC1 and 10 nM DNA-4.

complex in that side chain and backbone interactions are responsible for ribose discrimination (*57*).

We would not expect steric interactions to play a major role in selectivity against araCTP. While araC contains a 2′-hydroxyl group, it points toward the major groove and would not interact with the steric gate that selects against ribose. NMR structures of araC in oligonucleotides reveal that the ribose ring forms the canonical 2′-endo pucker of a dC moiety, but small differences in the torsional angles lead to an increase in helical bending (*58*−*61*). The changes in conformation do not lead to large decreased rates of incorporation.

The 2′-fluoro substituents of FdCTP and dFdCTP increase the electron density at that position, increase the physical size, and change the puckering of the ribose ring (*62*). While DNA has the 2′-endo conformation, dFdC has the 3′-endo conformation (*63*). 2′-(*R*)-Fluoronucleosides with the stereochemistry opposite of FdCTP exhibit a O4′-endo pucker (*64*, *65*). The conformational consequences of the 2′-(*S*)-fluoronucleosides, that we employed, are not known. Despite these differences, the k_{pol}/K_d^{dNTP} of dFdCTP is only 10-fold less than that of dCTP. The 10-fold reduction in k_{pol}/K_d of dFdCTP can be due to one or a combination of these effects.

FdCTP shows dramatic differences depending on DNA sequence. FdCTP is a good substrate with DNA-1 but a very poor substrate with DNA-3 due to a decreased k_{pol} value. Local DNA sequences affect DNA polymerases. For instance, sequence-dependent mutational frequencies have been noted for pol β (*66*). Thus, the local DNA sequence must introduce structural changes in the polymerase−DNA interactions that affect fidelity as well as selectivity of nucleotides modified at the 2′-position.

The mechanism by which dFdC and araC can affect the dissociation of DNA from pol β is not readily apparent. The working hypothesis is that araC and dFdC can induce sequence-specific conformations that affect the binding affinity of the DNA. The tight binding of pol β to the nicked araC and dFdC DNA may inhibit ligation of the nick, thereby extending the lifetime of the potentially cytotoxic nicked DNA. Thus, the tight binding of araC and dFdC nicked DNA to pol β may have implications in vivo.

Ligation. Enzymatic ligation consists of four steps: (i) a catalytic lysine attacks the α-phosphate of ATP, generating a lysyl-AMP adduct and releasing pyrophosphate, (ii) the adenylylated ligase binds nicked DNA and (iii) transfers the AMP

group from lysine to the 5′-phosphate of the nick, and (iv) the 3′-hydroxyl of the nick then attacks the adenylylated 5′-phosphate, forming a phosphodiester bond and eliminating AMP. Human DNA ligase I and III discriminate strongly between a correctly paired versus a mispaired residue at the 3′-position of a nick in DNA (*67*). However, RNA on the 3′-end of the nick is well tolerated by ligase I (*68*). The crystal structure of human ligase I with nicked DNA showed that the 5′-phosphorylated end of the DNA substrate is positioned in the active site of ligase I by extensive interactions with the 5′-AMP group. In contrast, the 3′-OH end makes few interactions with the enzyme, and proper alignment is dependent on interstrand base pairing (*68*).

We found that for both T4 ligase and ligase III/XRCC1 the identity of the nucleotide analogue had minimal effect on the rate of reaction. Ligase III/XRCC1 was affected to a greater extent, and the effect was dependent on the dC analogue and the sequence. For example, with DNA-2, ligation of araC was inhibited 50-fold and dFdC was inhibited 330-fold, while in DNA-4, ligation of dFdC was not inhibited while ligation of araC was inhibited 20-fold.

The mechanism of inhibition was not evaluated but may include a decreased rate of nick sealing (step iv described above). It is in this step that the dC analogue would actively take part in the reaction. The 2′-substitutions affect the conformation of the ribose ring and consequently the orientation of the 3′-hydroxyl. The position of this hydroxyl is important because it acts as the nucleophile in the final nick sealing step. Small alterations in this position should significantly affect reactivity.

Potential Relevance to Clinical Toxicity. Our results indicate that pol β has considerable opportunity to incorporate dFdC and araC into the DNA. This can be a mechanism by which araC and dFdC are incorporated into the DNA during toxicity and can result due to decreased ability of ligase III to seal the nick leaving a single-strand break that can prove fatal to the cell. Several tumor tissues have been shown to have increased expression of pol β (*32*), which may provide more opportunity for the incorporation of gemcitabine into the genome via the BER pathway and thus make it more cytotoxic in individuals with these types of tumors.

ACKNOWLEDGMENT

The NMR spectra were performed at the Penn State College of Medicine Solution Phase NMR Facility.

SUPPORTING INFORMATION AVAILABLE

Synthesis and characterization of dFdCTP and purity of DNA polymerase β. This material is available free of charge via the Internet at http://pubs.acs.org.

REFERENCES

1. Burnett, A. K., Milligan, D., Prentice, A. G., Goldstone, A. H., McMullin, M. F., Hills, R. K., and Wheatley, K. (2007) A comparison of low-dose cytarabine and hydroxyurea with or without all-trans retinoic acid for acute myeloid leukemia and high-risk myelodysplastic syndrome in patients not considered fit for intensive treatment. *Cancer 109*, 1114–1124.
2. Crino, L., Mosconi, A. M., Scagliotti, G., Selvaggi, G., Novello, S., Rinaldi, M., Della, G. M., Gridelli, C., Rossi, A., Calandri, C., De Marinis, F., Noseda, M., and Tonato, M. (1999) Gemcitabine as second-line treatment for advanced non-small-cell lung cancer: a phase II trial. *J. Clin. Oncol. 17*, 2081–2085.
3. Tempero, M., Plunkett, W., Ruiz, v. H. V., Hainsworth, J., Hochster, H., Lenzi, R., and Abbruzzese, J. (2003) Randomized phase II comparison of dose-intense gemcitabine: thirty-minute infusion and fixed dose rate infusion in patients with pancreatic adenocarcinoma. *J. Clin. Oncol. 21*, 3402–3408.
4. Burris, H. A., III, Moore, M. J., Andersen, J., Green, M. R., Rothenberg, M. L., Modiano, M. R., Cripps, M. C., Portenoy, R. K., Storniolo, A. M., Tarassoff, P., Nelson, R., Dorr, F. A., Stephens, C. D., and Von Hoff, D. D. (1997) Improvements in survival and clinical benefit with gemcitabine as first-line therapy for patients with advanced pancreas cancer: a randomized trial. *J. Clin. Oncol. 15*, 2403–2413.
5. Hensley, M. L., Correa, D. D., Thaler, H., Wilton, A., Venkatraman, E., Sabbatini, P., Chi, D. S., Dupont, J., Spriggs, D., and Aghajanian, C. (2006) Phase I/II study of weekly paclitaxel plus carboplatin and gemcitabine as first-line treatment of advanced-stage ovarian cancer: pathologic complete response and longitudinal assessment of impact on cognitive functioning. *Gynecol. Oncol. 102*, 270–277.
6. Morandi, P. (2006) Biological agents and gemcitabine in the treatment of breast cancer. *Ann. Oncol. 17* (Suppl. 5), v177–v180.
7. Carmichael, J., and Walling, J. (1996) Phase II activity of gemcitabine in advanced breast cancer. *Semin. Oncol. 23*, 77–81.
8. Nabhan, C., Krett, N., Gandhi, V., and Rosen, S. (2001) Gemcitabine in hematologic malignancies. *Curr. Opin. Oncol. 13*, 514–521.
9. Sallah, S., Wan, J. Y., and Nguyen, N. P. (2001) Treatment of refractory T-cell malignancies using gemcitabine. *Br. J. Haematol. 113*, 185–187.
10. Gandhi, V., Mineishi, S., Huang, P., Chapman, A. J., Yang, Y., Chen, F., Nowak, B., Chubb, S., Hertel, L. W., and Plunkett, W. (1995) Cytotoxicity, metabolism, and mechanisms of action of 2′,2′-difluorodeoxyguanosine in Chinese hamster ovary cells. *Cancer Res. 55*, 1517–1524.
11. Huang, P., Chubb, S., Hertel, L. W., Grindey, G. B., and Plunkett, W. (1991) Action of 2′,2′-difluorodeoxycytidine on DNA synthesis. *Cancer Res. 51*, 6110–6117.
12. Iwasaki, H., Huang, P., Keating, M. J., and Plunkett, W. (1997) Differential incorporation of ara-C, gemcitabine, and fludarabine into replicating and repairing DNA in proliferating human leukemia cells. *Blood 90*, 270–278.
13. Heinemann, V., Hertel, L. W., Grindey, G. B., and Plunkett, W. (1988) Comparison of the cellular pharmacokinetics and toxicity of 2′,2′-difluorodeoxycytidine and 1-beta-D-arabinofuranosylcytosine. *Cancer Res. 48*, 4024–4031.
14. Shao, J., Zhou, B., Chu, B., and Yen, Y. (2006) Ribonucleotide reductase inhibitors and future drug design. *Curr. Cancer Drug Targets 6*, 409–431.
15. Wang, J., Lohman, G. J. S., and Stubbe, J. (2009) Mechanism of inactivation of human ribonucleotide reductase with p53R2 by gemcitabine 5′-diphosphate. *Biochemistry 48*, 11612–11621.
16. Artin, E., Wang, J., Lohman, G. J. S., Yokoyama, K., Yu, G., Griffin, R. G., Bar, G., and Stubbe, J. (2009) Insight into the mechanism of inactivation of ribonucleotide reductase by gemcitabine 5′-diphosphate in the presence or absence of reductant. *Biochemistry 48*, 11622–11629.
17. Pourquier, P., Takebayashi, Y., Urasaki, Y., Gioffre, C., Kohlhagen, G., and Pommier, Y. (2000) Induction of topoisomerase I cleavage complexes by 1-beta-D-arabinofuranosylcytosine (ara-C) in vitro and in ara-C-treated cells. *Proc. Natl. Acad. Sci. U.S.A. 97*, 1885–1890.
18. Pourquier, P., Gioffre, C., Kohlhagen, G., Urasaki, Y., Goldwasser, F., Hertel, L. W., Yu, S., Pon, R. T., Gmeiner, W. H., and Pommier, Y. (2002) Gemcitabine (2′,2′-difluoro-2′-deoxycytidine), an antimetabolite that poisons topoisomerase I. *Clin. Cancer Res. 8*, 2499–2504.
19. Richardson, K. A., Vega, T. P., Richardson, F. C., Moore, C. L., Rohloff, J. C., Tomkinson, B., Bendele, R. A., and Kuchta, R. D. (2004) Polymerization of the triphosphates of AraC, 2′,2′-difluorodeoxycytidine (dFdC) and OSI-7836 (T-araC) by human DNA polymerase alpha and DNA primase. *Biochem. Pharmacol. 68*, 2337–2346.
20. Jiang, H. Y., Hickey, R. J., Abdel-Aziz, W., and Malkas, L. H. (2000) Effects of gemcitabine and araC on in vitro DNA synthesis mediated by the human breast cell DNA synthesome. *Cancer Chemother. Pharmacol. 45*, 320–328.
21. Fowler, J. D., Brown, J. A., Johnson, K. A., and Suo, Z. (2008) Kinetic investigation of the inhibitory effect of gemcitabine on DNA polymerization catalyzed by human mitochondrial DNA polymerase gamma. *J. Biol. Chem. 283*, 15339–15348.
22. Shi, Z., Azuma, A., Sampath, D., Li, Y. X., Huang, P., and Plunkett, W. (2001) S-phase arrest by nucleoside analogues and abrogation of survival without cell cycle progression by 7-hydroxystaurosporine. *Cancer Res. 61*, 1065–1072.
23. Ewald, B., Sampath, D., and Plunkett, W. (2007) H2AX phosphorylation marks gemcitabine-induced stalled replication forks and their

collapse upon S-phase checkpoint abrogation. *Mol. Cancer Ther. 6*, 1239–1248.
24. Chen, Y. W., Cleaver, J. E., Hanaoka, F., Chang, C. F., and Chou, K. M. (2006) A novel role of DNA polymerase eta in modulating cellular sensitivity to chemotherapeutic agents. *Mol. Cancer Res. 4*, 257–265.
25. Liu, G., and Chen, X. (2006) DNA polymerase eta, the product of the xeroderma pigmentosum variant gene and a target of p53, modulates the DNA damage checkpoint and p53 activation. *Mol. Cell. Biol. 26*, 1398–1413.
26. Crul, M., van Waardenburg, R. C. A. M., Bocxe, S., van Eijndhoven, M. A. J., Pluim, D., Beijnen, J. H., and Schellens, J. H. M. (2003) DNA repair mechanisms involved in gemcitabine cytotoxicity and in the interaction between gemcitabine and cisplatin. *Biochem. Pharmacol. 65*, 275–282.
27. Pelicano, H., Carney, D., and Huang, P. (2004) ROS stress in cancer cells and therapeutic implications. *Drug Resist. Updates 7*, 97–110.
28. Kow, Y. W. (2002) Repair of deaminated bases in DNA. *Free Radical Biol. Med. 33*, 886–893.
29. Caulfield, J. L., Wishnok, J. S., and Tannenbaum, S. R. (1998) Nitric oxide-induced deamination of cytosine and guanine in deoxynucleosides and oligonucleotides. *J. Biol. Chem. 273*, 12689–12695.
30. Geller, H. M., Cheng, K. Y., Goldsmith, N. K., Romero, A. A., Zhang, A. L., Morris, E. J., and Grandison, L. (2001) Oxidative stress mediates neuronal DNA damage and apoptosis in response to cytosine arabinoside. *J. Neurochem. 78*, 265–275.
31. Conklin, K. A. (2004) Chemotherapy-associated oxidative stress: impact on chemotherapeutic effectiveness. *Integr. Cancer Ther. 3*, 294–300.
32. Albertella, M. R., Lau, A., and O'Connor, M. J. (2005) The overexpression of specialized DNA polymerases in cancer. *DNA Repair 4*, 583–593.
33. Lamarche, B. J., Showalter, A. K., and Tsai, M. D. (2005) An error-prone viral DNA ligase. *Biochemistry 44*, 8408–8417.
34. Zhao, X., Muller, J. G., Halasyam, M., David, S. S., and Burrows, C. J. (2007) In vitro ligation of oligodeoxynucleotides containing C8-oxidized purine lesions using bacteriophage T4 DNA ligase. *Biochemistry 46*, 3734–3744.
35. Ludwig, J. (1981) A new route to nucleoside 5′-triphosphates. *Acta Biochim. Biophys. Acad. Sci. Hung. 16*, 131–133.
36. Opresko, P. L., Shiman, R., and Eckert, K. A. (2000) Hydrophobic interactions in the hinge domain of DNA polymerase beta are important but not sufficient for maintaining fidelity of DNA synthesis. *Biochemistry 39*, 11399–11407.
37. Kretulskie, A. M., and Spratt, T. E. (2006) Structure of purine-purine mispairs during misincorporation and extension by *E. coli* DNA polymerase I. *Biochemistry 45*, 3740–3746.
38. Nick McElhinny, S. A., and Ramsden, D. A. (2003) Polymerase mu is a DNA-directed DNA/RNA polymerase. *Mol. Cell. Biol. 23*, 2309–2315.
39. Ruiz, J. F., Juarez, R., Garcia-Diaz, M., Terrados, G., Picher, A. J., Gonzalez-Barrera, S., Fernandez de Henestrosa, A. R., and Blanco, L. (2003) Lack of sugar discrimination by human Pol mu requires a single glycine residue. *Nucleic Acids Res. 31*, 4441–4449.
40. Showalter, A. K., and Tsai, M. D. (2002) A reexamination of the nucleotide incorporation fidelity of DNA polymerases. *Biochemistry 41*, 10571–10576.
41. Roettger, M. P., Bakhtina, M., and Tsai, M. D. (2008) Mismatched and matched dNTP incorporation by DNA polymerase beta proceed via analogous kinetic pathways. *Biochemistry 47*, 9718–9727.
42. Tang, K. H., Niebuhr, M., Tung, C. S., Chan, H. C., Chou, C. C., and Tsai, M. D. (2008) Mismatched dNTP incorporation by DNA polymerase beta does not proceed via globally different conformational pathways. *Nucleic Acids Res. 36*, 2948–2957.
43. Ahn, J., Kraynov, V. S., Zhong, X., Werneburg, B. G., and Tsai, M. D. (1998) DNA polymerase beta: effects of gapped substrates on dNTP specificity, fidelity, processivity and conformational changes. *Biochem. J. 331*, 79–87.
44. Vande Berg, B. J., Beard, W. A., and Wilson, S. H. (2001) DNA structure and aspartate 276 influence nucleotide binding to human DNA polymerase beta. Implication for the identity of the rate-limiting conformational change. *J. Biol. Chem. 276*, 3408–3416.
45. DeLucia, A. M., Chaudhuri, S., Potapova, O., Grindley, N. D. F., and Joyce, C. M. (2006) The properties of steric gate mutants reveal different constraints within the active sites of Y-family and A-family DNA polymerases. *J. Biol. Chem. 281*, 27286–27291.
46. Mikita, T., and Beardsley, G. P. (1988) Functional consequences of the arabinosylcytosine structural lesion in DNA. *Biochemistry 27*, 4698–4705.
47. Bakhtina, M., Roettger, M. P., and Tsai, M. D. (2009) Contribution of the reverse rate of the conformational step to polymerase beta fidelity. *Biochemistry 48*, 3197–3208.
48. Bakhtina, M., Roettger, M. P., Kumar, S., and Tsai, M. D. (2007) A unified kinetic mechanism applicable to multiple DNA polymerases. *Biochemistry 46*, 5463–5472.
49. DeLucia, A. M., Grindley, N. D. F., and Joyce, C. M. (2003) An error-prone family Y DNA polymerase (DinB homolog from *Sulfolobus solfataricus*) uses a "steric gate" residue for discrimination against ribonucleotides. *Nucleic Acids Res. 31*, 4129–4137.
50. Astatke, M., Ng, K., Grindley, N. D., and Joyce, C. M. (1998) A single side chain prevents *Escherichia coli* DNA polymerase I (Klenow fragment) from incorporating ribonucleotides. *Proc. Natl. Acad. Sci. U.S.A. 95*, 3402–3407.
51. Yang, G., Franklin, M., Li, J., Lin, T. C., and Konigsberg, W. (2002) A conserved Tyr residue is required for sugar selectivity in a pol alpha DNA polymerase. *Biochemistry 41*, 10256–10261.
52. Bonnin, A., Lsszaro, J. M., Blanco, L., and Salas, M. (1999) A single tyrosine prevents insertion of ribonucleotides in the eukaryotic-type [phi]29 DNA polymerase. *J. Mol. Biol. 290*, 241–251.
53. Gardner, A. F., and Jack, W. E. (1999) Determinants of nucleotide sugar recognition in an archaeon DNA polymerase. *Nucleic Acids Res. 27*, 2545–2553.
54. Cases-Gonzalez, C. E., Gutierrez-Rivas, M., and Menendez-Arias, L. (2000) Coupling ribose selection to fidelity of DNA synthesis. *J. Biol. Chem. 275*, 19759–19767.
55. Pelletier, H. (1994) Polymerase structures and mechanism. *Science 266*, 2025–2026.
56. Beard, W. A., and Wilson, S. H. (1998) Structural insights into polymerase beta fidelity: hold tight if you want it right. *Chem. Biol. 5*, R7–R13.
57. Brown, T., Hunter, W. N., Kneale, G., and Kennard, O. (1986) Molecular structure of the G·A base pair in DNA and its implications for the mechanism of transversion mutations. *Proc. Natl. Acad. Sci. U.S.A. 83*, 2402–2406.
58. Gmeiner, W. H., Skradis, A., Pon, R. T., and Liu, J. (1998) Cytarabine-induced destabilization of a model Okazaki fragment. *Nucleic Acids Res. 26*, 2359–2365.
59. Schweitzer, B. I., Mikita, T., Kellogg, G. W., Gardner, K. H., and Beardsley, G. P. (1994) Solution structure of a DNA dodecamer containing the anti-neoplastic agent arabinosylcytosine: combined use of NMR, restrained molecular dynamics, and full relaxation matrix refinement. *Biochemistry 33*, 11460–11475.
60. Pieters, J. M., de Vroom, E., van der Marel, G. A., van Boom, J. H., Koning, T. M., Kaptein, R., and Altona, C. (1990) Hairpin structures in DNA containing arabinofuranosylcytosine. A combination of nuclear magnetic resonance and molecular dynamics. *Biochemistry 29*, 788–799.
61. Pieters, J. M., de Vroom, E., van der Marel, G. A., van Boom, J. H., and Altona, C. (1989) Conformational consequences of the incorporation of arabinofuranosylcytidine in DNA. An NMR study of the DNA fragments d(CGCTAGCG) and d(CGaCTAGCG) in solution. *Eur. J. Biochem. 184*, 415–425.
62. Smart, B. E. (2001) Fluorine substituent effects (on bioactivity). *J. Fluorine Chem. 109*, 3–11.
63. Konerding, D., James, T. L., Trump, E., Soto, A. M., Marky, L. A., and Gmeiner, W. H. (2002) NMR structure of a gemcitabine-substituted model Okazaki fragment. *Biochemistry 41*, 839–846.
64. Lee, S., Bowman, B. R., Ueno, Y., Wang, S., and Verdine, G. L. (2008) Synthesis and structure of duplex DNA containing the genotoxic nucleobase lesion N7-methylguanine. *J. Am. Chem. Soc. 130*, 11570–11571.
65. Bowman, B. R., Lee, S., Wang, S., and Verdine, G. L. (2008) Structure of the *E. coli* DNA glycosylase AlkA bound to the ends of duplex DNA: a system for the structure determination of lesion-containing DNA. *Structure 16*, 1166–1174.
66. Osheroff, W. P., Jung, H. K., Beard, W. A., Wilson, S. H., and Kunkel, T. A. (1999) The fidelity of DNA polymerase beta during distributive and processive DNA synthesis. *J. Biol. Chem. 274*, 3642–3650.
67. Bhagwat, A. S., Sanderson, R. J., and Lindahl, T. (1999) Delayed DNA joining at 3′ mismatches by human DNA ligases. *Nucleic Acids Res. 27*, 4028–4033.
68. Pascal, J. M., O'Brien, P. J., Tomkinson, A. E., and Ellenberger, T. (2004) Human DNA ligase I completely encircles and partially unwinds nicked DNA. *Nature 432*, 473–478.